Int. J. Solids Structures, 1969, Vol. 5, pp. 767 to 780. Pergamon Press. Printed in Great Britain

ON THE USE OF A SPRING–MASS TO APPROXIMATE A BAR–MASS SYSTEM SUBJECTED TO A RECTANGULAR FORCE PULSE†

A. E. SEIGEL‡ and R. H. WASER

U.S. Naval Ordnance Laboratory, White Oak, Silver Spring, Maryland

Abstract—An analysis with experimental confirmation of a bar–mass system is described. The bar is built in at one end and has a rigid mass connected to the other end. To the rigid mass is applied a rectangular-step-force pulse of magnitude such that the bar is *elastically* deformed. The resulting behavior of the bar–mass system is calculated with the assumption that the stresses in the bar are one-dimensional. These calculations yield the fact that the bar–mass system experiences forces that are significantly larger than those experienced by an equivalent spring–mass approximation in the case of short pulse duration and/or magnitude of mass. The calculated results are confirmed by experiments performed on a bar–mass system.

NOMENCLATURE

A	cross-sectional area of bar
a	Lagrangian length coordinate
E	Young's modulus
ε	strain
F	force
F_{max}	maximum force at the built-in end of a system
k	spring constant
l	length of bar
M	mass of rigid mass
m	mass of bar
ρ_0	initial mass density
σ	stress
T_n	natural period
t	time
t'	dimensionless time
Δt	force pulse duration
u	particle velocity
x	distance coordinate

1. INTRODUCTION

IN ORDER to calculate the stresses experienced by a structure subjected to rapidly applied loads, the structure is often approximated as a system of spring-masses (see, for example, [1]). The structure of interest here is one of the simplest, the so-called "bar–mass system." It consists of a bar of mass, m, built in at one end and connected to a rigid of mass, M, at the other end. The spring-mass approximation in this instance consists of a *massless* spring having the elastic characteristics of the bar; this spring is similarly built in at one end, but at the other end is connected a rigid mass increased in mass to account for the

† This paper is partly based on a thesis submitted by Mr. R. H. Waser to the Mechanical Engineering Department of the University of Maryland as partial fulfillment of the requirements for the degree of Master of Science.

‡ Lecturer, Mechanical Engineering and Aerospace Engineering Departments, University of Maryland.

inertia of the bar to a value of $M+m/3$.† The bar–mass system and the spring–mass approximation are shown in Fig. 1. To be examined is the case of suddenly applied rectangular force of duration Δt acting on the rigid mass as depicted in Fig. 2. The magnitude of the force is assumed to be limited such that the bar is *elastically* deformed. The question

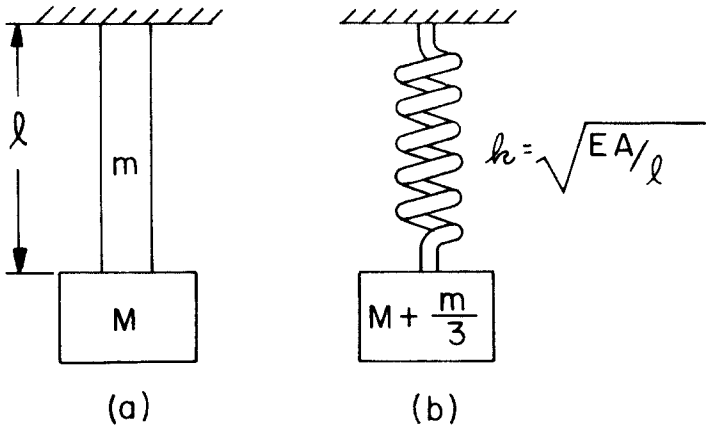

FIG. 1. Bar–mass system (a) and spring-mass approximation (b).

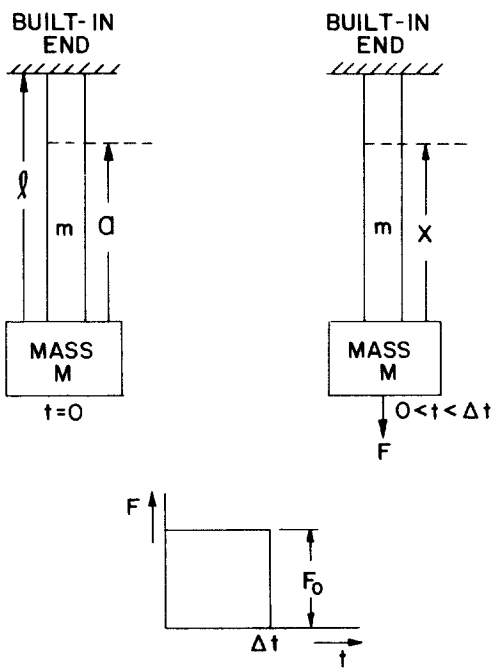

FIG. 2. Bar–mass system and applied force pulse.

† This spring–mass approximation yields a natural period, T_n, which is in good agreement with the fundamental period of the bar–mass system as calculated from the one-dimensional stress-wave theory (see, for example, [2] and [3]).

to be answered in this study is the following: How accurately are the maximum forces experienced by the bar–mass system under such a rectangular loading calculated from the use of the spring–mass approximation?

The behavior of a spring–mass system subjected to a rectangular pulse is well known (see [4], for example). The spring, being massless, experiences the same force throughout its length. The maximum force experienced by the spring, and hence at the built-in support, depends on the pulse duration as shown in Fig. 3. However, the behavior of the bar–mass system is not generally known but may be calculated by assuming that the stress in the bar is one-dimensional.†

With the one-dimensional assumption the elastic behavior of the bar–mass system was calculated for the entire range of pulse duration Δt, and mass ratio m/M. These calculations are outlined below. The results of these calculations, and particularly the calculated maximum forces, were then compared to the spring–mass approximation. To confirm the calculations an experimental check of one of the calculated cases was performed.

2. BAR–MASS EQUATIONS

The bar–mass system is visualized as shown in Fig. 2. The equation of motion of the mass, M, considered as a rigid body, see Fig. 4, is

$$M\frac{du_1}{dt} = \sigma_1 A - F(t) \tag{1}$$

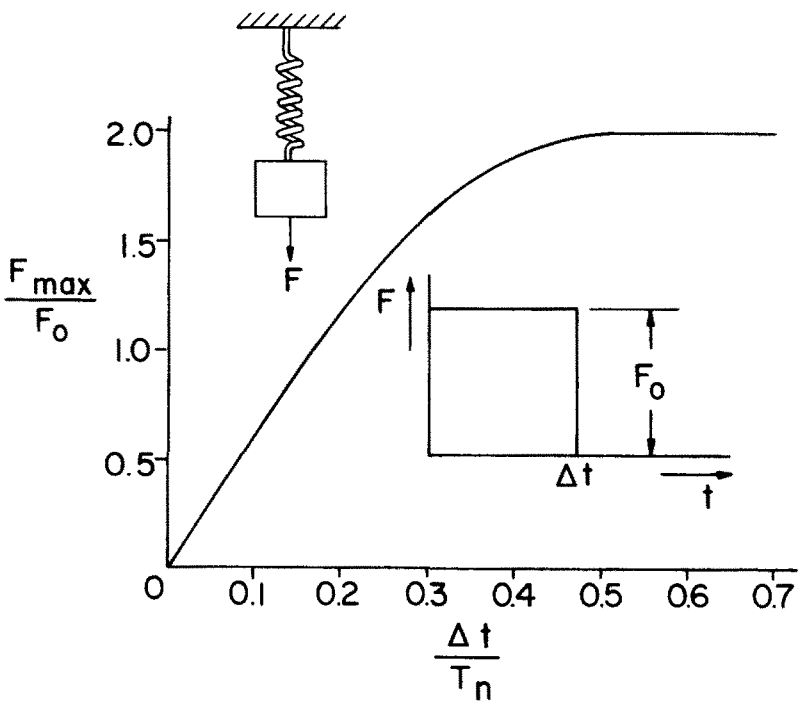

FIG. 3. F_{max}/F_0 vs. force pulse duration for a spring-mass system

† One-dimensional wave-propagation problems of the elastic behavior of a bar were treated long ago. For example, the longitudinal impact of a rigid mass with a bar, a problem similar to the one of interest here, was treated in 1883 [7] (see also Love [5] and Goldsmith [6]).

where M is the mass of the rigid body, u_1 is the velocity of the mass, $\sigma_1 A$ is the force exerted on the mass by the bar, and $F(t)$ is the force applied to the rigid body.

The behavior of the bar is governed by the continuity and momentum equations which with the assumption of one-dimensionality take the following form in the Lagrangian coordinate system:

$$\frac{\partial x}{\partial a} = \varepsilon + 1$$
$$\frac{\partial \sigma}{\partial a} = \rho_0 \frac{\partial u}{\partial t} \tag{2}$$

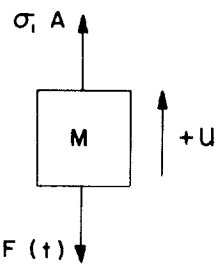

FIG. 4. Free body diagram for rigid mass.

where x, ε, σ, ρ_0, and u are the distance coordinate, strain, stress, initial mass density, and particle velocity, respectively; the Lagrangian coordinate "a" is measured in the unstrained bar as shown in Fig. 2.

For one-dimensional elastic deformations the stress–strain relation is simply

$$\frac{\sigma}{\varepsilon} = E \tag{3}$$

where E is Young's modulus.

Equations (2) and (3) may be transformed into many forms of the classical wave equation with constant sound speed. Here it was chosen to put these equations in a form suitable for the method of characteristics; thus, by following Courant and Friedrichs [8], equations (2) and (3) become the characteristic equations

$$\frac{\partial}{\partial t}\left(u \mp \frac{\sigma}{\sqrt{E\rho_0}}\right) \pm \sqrt{\frac{E}{\rho_0}} \frac{\partial}{\partial a}\left(u \mp \frac{\sigma}{\sqrt{E\rho_0}}\right) = 0. \tag{4}$$

At the position where the bar and mass are joined (i.e. at the $a = 0$ position)

$$\sigma = \sigma_1,$$

and (5)

$$u = u_1.$$

At the built-in end of the bar (i.e. at $a = l$)

$$u = 0. \tag{6}$$

Equations (1, 4–6) are sufficient to determine the behavior of the bar–mass system for a given applied force, $F(t)$.

A characteristic diagram in the a–t plane which depicts the paths of disturbances (i.e. the characteristic lines) appears as shown in Fig. 5. Each of the regions I, II, III, etc.

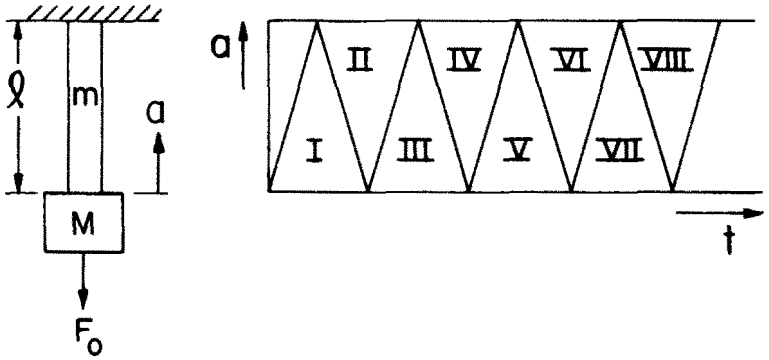

FIG. 5. Bar–mass characteristic diagram.

is bounded by the first disturbance and its reflections from the built-in end and from the rigid body. In each of these regions it develops that through the use of equations (1, 4–6), closed-form analytic expressions may be obtained for stress, displacement, velocity, etc., for the case of an applied rectangular force. [These resemble the equations obtained by Love [5] (see also [6]).] These expressions were numerically evaluated by hand to obtain the results discussed below.

3. RESULTS OF CALCULATIONS

Figure 6 indicates the calculated maximum forces experienced at each end of the bar when the constant force is maintained indefinitely ($\Delta t = \infty$). As seen from the figure, the maximum force experienced at the fixed end of the bar ($a = l$) is always greater than 2 (except at m/M equal to zero and infinity). This is an unexpected result since the spring–mass analogy yields a maximum force ratio of 2. It is reasoned that this occurs because of the inertia of the bar. The bar, having attained a velocity as a result of being pulled by a rigid mass, continues its motion because of its inertia beyond where an inertialess spring would stop. This result differs from that of the spring-mass analogy (for which the maximum force ratio is equal to two), because the inertia at the bar is not properly accounted for in the analogy. An improved representation of the bar mass would be to represent the

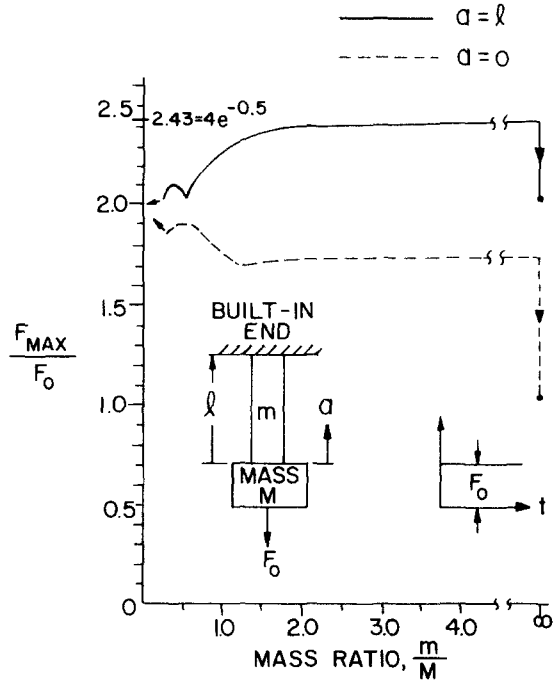

FIG. 6. Calculated F_{max}/F_0 vs. mass ratio for a step-pulse of infinite duration.

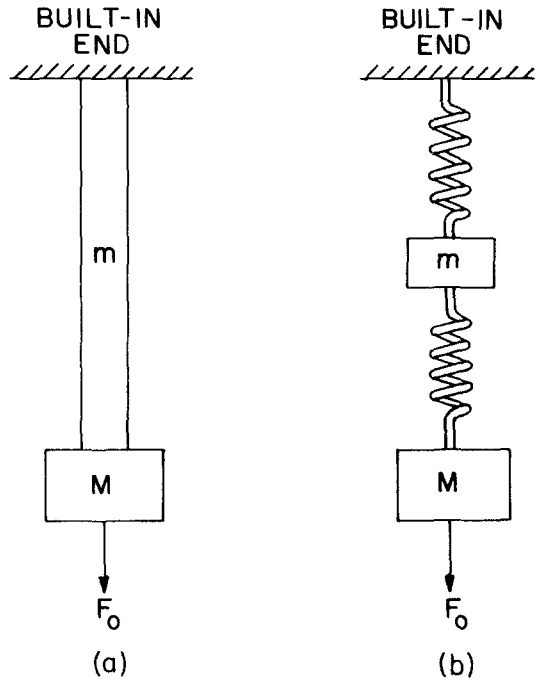

FIG. 7. Bar itself of bar–mass system (a) represented as spring–mass in (b).

bar itself as a spring mass, as shown in Fig. 7. In this case, calculation indicates that the force at the built-in end will exceed the value of twice the applied force.

Figure 8 illustrates the calculated force–time history at the built-in end for several m/M ratios for the constant force indefinitely maintained case. It is to be noted that the time duration during which the force is greater than 2 decreases with increasing m/M ratios.

For the particular case of m/M ratio equal to 2, the forces at each end of the bar and the rigid mass displacement are plotted in Fig. 9. It is noted that the displacement curve appears somewhat harmonic; the force histories are definitely nonharmonic.

If the force applied to the rigid mass is suddenly removed after a time, Δt, the disturbance wave originating upon this removal will decrease the force in each part of the bar that it passes through. Until the time at which the removal pulse disturbance reaches a given point in the bar (this time being Δt plus $a/\sqrt{E/\rho_0}$), the continuous pulse analytic expressions are still applicable. The results of the calculations for the finite length pulse case are shown in Fig. 10 which is a plot of F_{max}/F_0 vs. $\Delta t/T_n$ for various m/M ratios. The

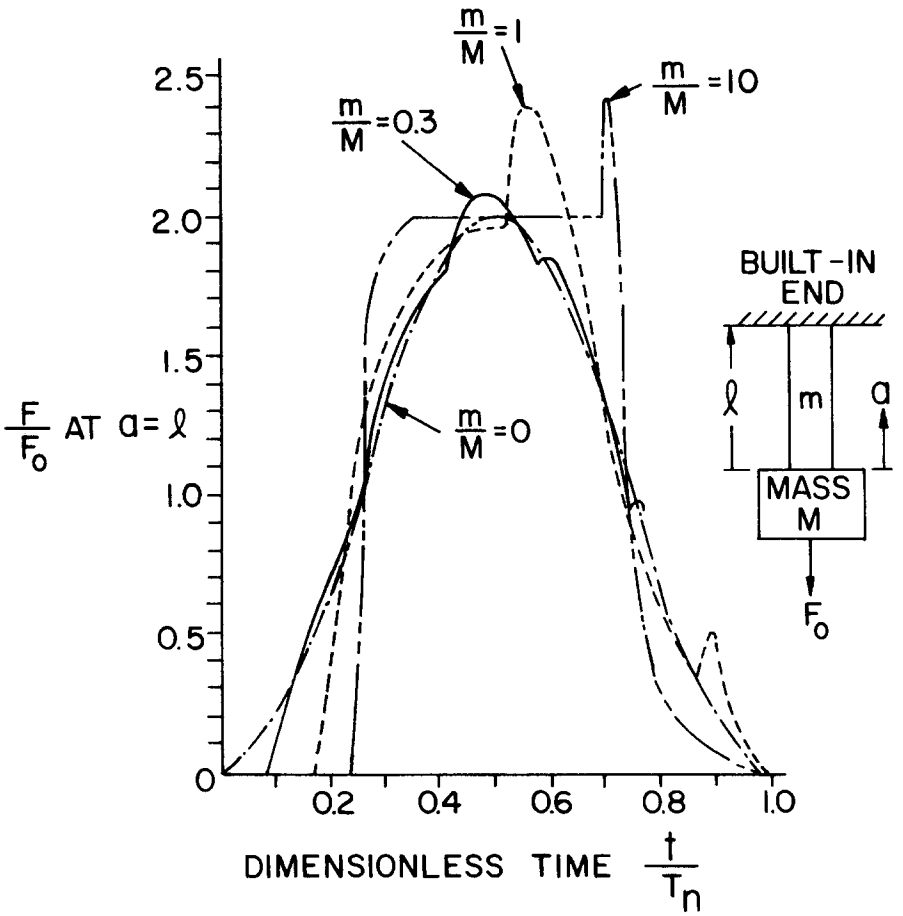

FIG. 8. Calculated F/F_0 vs. time at $a = l$ for a step-pulse of infinite duration.

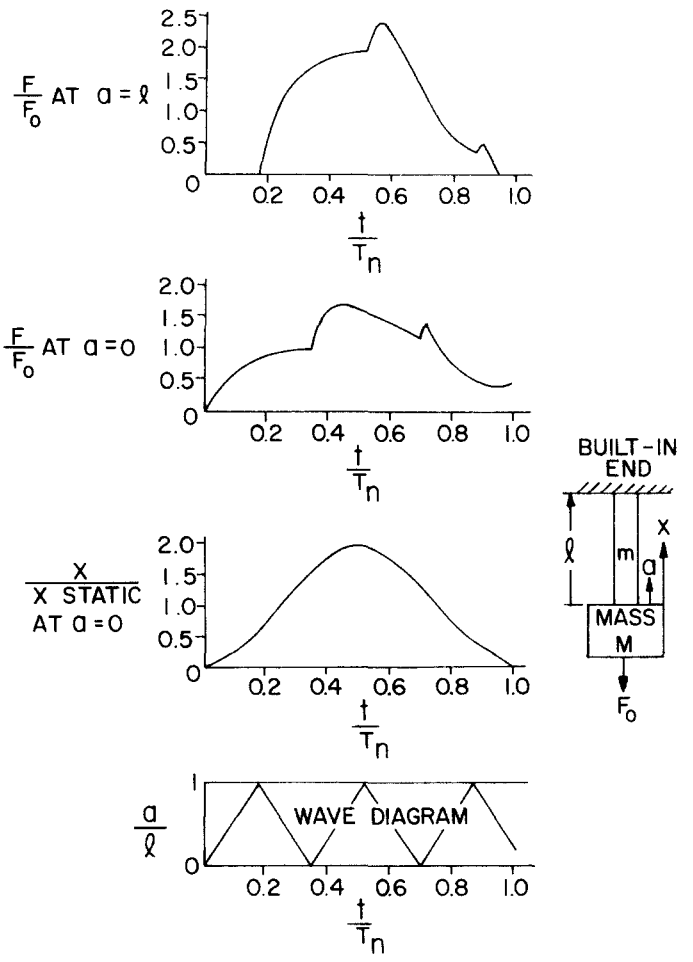

FIG. 9. Calculated forces and displacements vs. time for a step-pulse of infinite duration, $m/M = 2$.

m/M equal to zero curve in this figure corresponds to the spring–mass system. It is seen that there is considerable difference between the spring–mass case and the larger ratio m/M bar–mass cases. *In all cases the spring–mass approximation yields lower forces than actually occur in the bar–mass system.*

The error resulting from the use of the spring–mass approximation is more clearly seen from Fig. 11. This figure is a plot of the error in F_{max}/F_0 vs. the dimensionless pulse duration, $\Delta t/T_n$, for various m/M ratios. It is seen that large errors will result from the use of the spring–mass approximation in the case of short-duration pulses and large m/M ratios.

4. EXPERIMENTAL CONFIRMATION

To verify the results of the calculations, experiments were performed using one particular mass ratio, m/M. (The same experiment was repeated eight times, yielding results consistent within 5 per cent.) The mass ratio chosen was 2, since the calculated F_{max}/F_0 for this mass ratio was 2·40, which is much above the value 2 obtained from the spring–mass

approximation and which is close to the theoretical calculated maximum of 2·43. Because of the experimental difficulty of suddenly applying a force to a bar–mass system, the experiment involved instead the sudden release of a force from the bar–mass system. That the calculated case of the sudden application of a force is equivalent to the experimental case of the sudden release of a force becomes evident if one uses in the equations describing the experimental case the variables u' and σ' defined as follows:

$$u' = -u$$

$$\sigma' = F_0/A - \sigma.$$

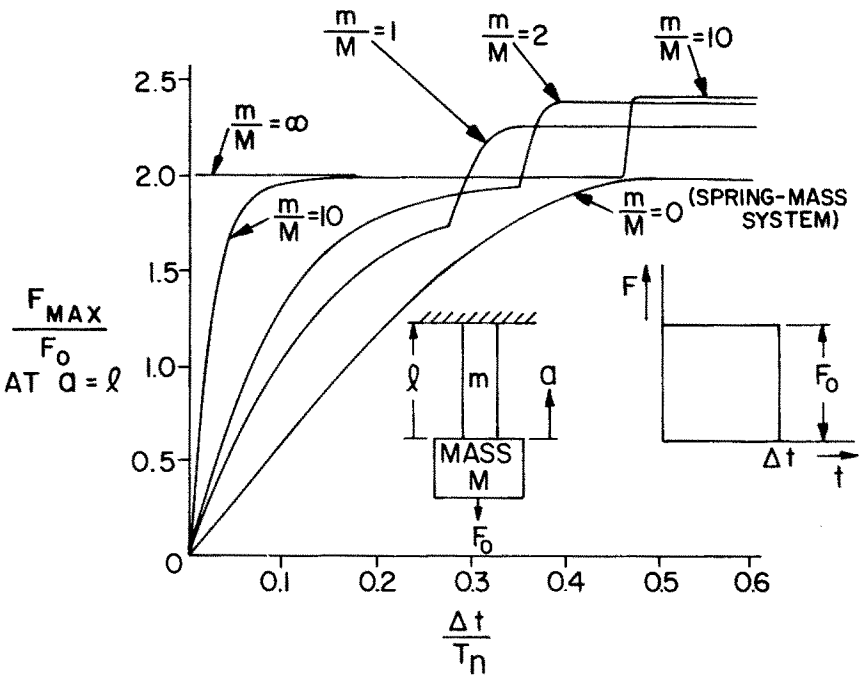

FIG. 10. Calculated F_{max}/F_0 at $a = l$ vs. force pulse duration.

With these redefined variables used to describe the experimental case, both the initial conditions (at $t = 0$) and the equations describing the motion of the bar and rigid mass at all subsequent times ($t > 0$) are identical for the two cases. The two situations are compared in Fig. 12.†

The experimental bar–mass apparatus at a time equal to zero appeared as shown in Fig. 13. The length and material (tungsten) of the rigid mass were chosen relative to the length and material (glass) of the bar so that disturbances would travel back and forth in the rigid mass about 32 times as fast as in the glass bar; thus, effectively, the tungsten

† The bar–mass system is pictured inverted relative to the usual illustrations to make it appear like the actual experimental system which, of necessity, was inverted (see Fig. 13).

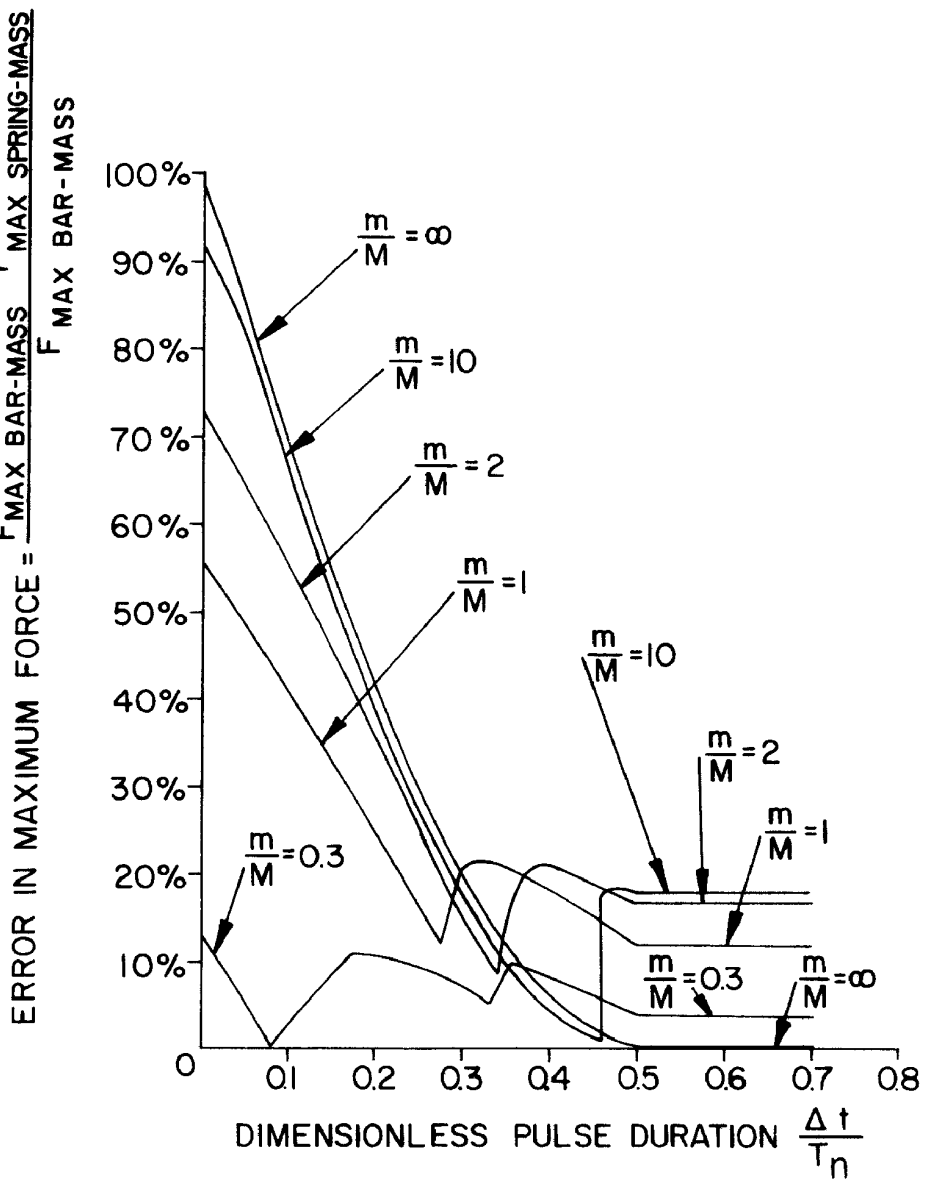

FIG. 11. Calculated error in maximum force at $a = l$ from use of spring–mass approximation.

rigid mass approximates a true rigid body relative to the glass bar. Glass was chosen as the bar material since it follows Hooke's law as closely as can be experimentally determined [9]. The rigid restraint at the built-in end was made of tungsten and of sufficient mass relative to the glass bar that it moved very little during the experiment.†

The physical characteristics of the bar–mass system used in the experiments are given in Appendix A.

† As mentioned below, the effect of the motion of the rigid restraint was calculated.

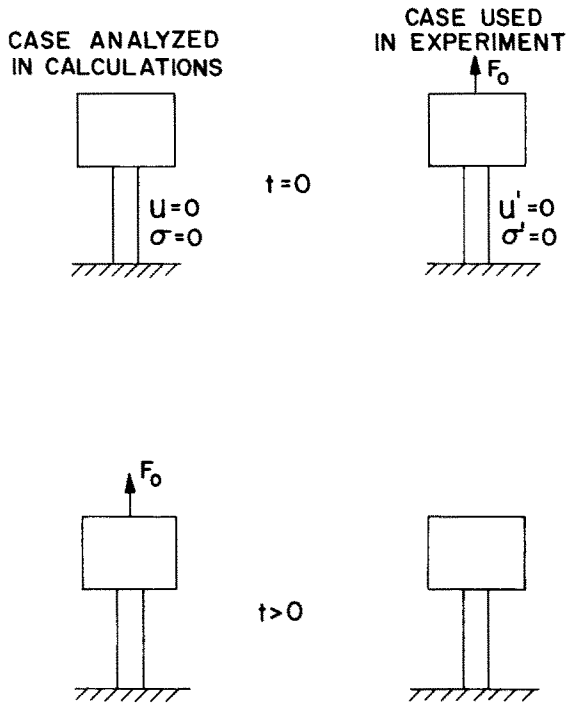

FIG. 12. Comparison of theoretical and experimental systems.

The complete assembly was supported by a nylon cord passed through a hole in the rigid mass and tied above to a support. In this manner, the system was initially stressed by a force equal to its total weight. Release of this force to provide the desired loading pulse was accomplished simply by burning the nylon cord supporting the system.

The force (or stress) experienced by the bar at its built-in end was obtained through the use of a pair of SR-4 type strain gages cemented to the bar. These gages were connected into a Wheatstone bridge in an additive manner so that any bending strains would be cancelled. The output from the bridge was displayed on an oscilloscope equipped with a camera for photographing the traces. The oscilloscope was triggered from a semiconductor strain gage mounted on the glass bar at the end nearest the rigid mass. In this manner, the oscilloscope sweep was initiated before the stress disturbance reached the strain gages at the built-in end of the bar.

A typical oscilloscope trace obtained from one of the eight tests is shown in Fig. 14. The horizontal trace at the bottom of the photograph was made with the bar–mass system in its initial prestressed condition, and the trace in the center of the picture was made after the force had been released and the system had stopped vibrating. Thus, the distance between these lines represents the magnitude of the force, F_0, applied to the system. The oscillatory trace in this figure is the measured force felt at the built-in end of the bar. The points superimposed on the oscilloscope trace in Fig. 14 are the results of calculations for this case which take into account the fact that the restraint at the built-in end of the bar is actually not absolutely rigid. It is seen that the agreement between the experiment and theory is quite good. The F'_{max}/F_0 ratio (where $F'_{max} = F_0 - F_{max}$) measured from the

photograph is 2·24, whereas 2·30 is the value calculated taking the non-rigidity of the restraint into account. (With an absolutely rigid restraint the value would have been 2·40.)

5. CONCLUDING REMARKS

This study indicates that the use of a spring–mass system to approximate the elastic behavior of a bar–mass system may result in very large errors; specifically, the maximum force as calculated from the spring–mass approximation is always less than, and is sometimes considerably less than that actually occurring in the bar–mass structure when it is subjected to a rectangular force pulse.

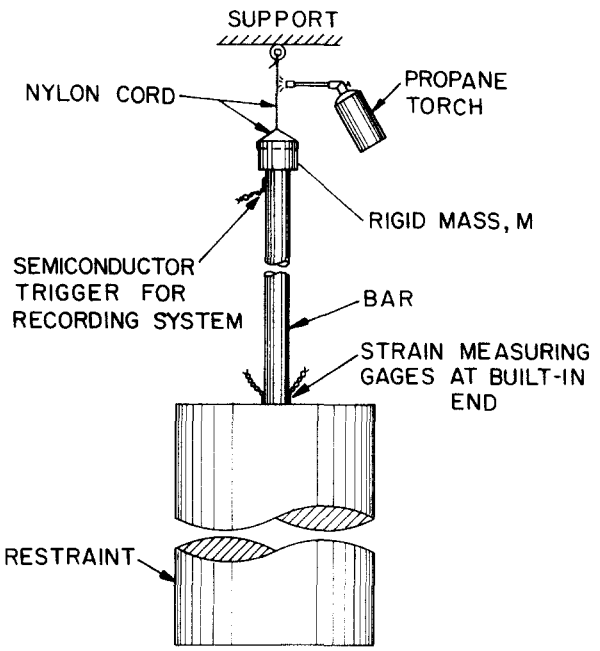

FIG. 13. Experimental bar–mass system.

As seen from Fig. 11, the error in maximum force resulting from use of the spring–mass approximation depends on the time duration of the pulse and the mass ratio m/M. When the pulse duration is short and the mass ratio large, the error is large (e.g. at $\Delta t/T_n = 0{\cdot}1$, and $m/M = 2$, the error is 55 per cent), whereas the error becomes smaller with increasing pulse duration and decreasing mass ratio. (It is interesting to note that in the case of long-duration pulses the ratio of the force experienced to that applied is *greater* than 2 (going as high as 2·43) for the bar–mass system, whereas this ratio is exactly 2 for the spring–mass approximation.)

It is speculated that errors will similarly result from the use of the spring–mass approximation in cases where the applied force pulse is other than rectangular (e.g. triangular). For any type of pulse, however, the results of the use of spring–masses to approximate the

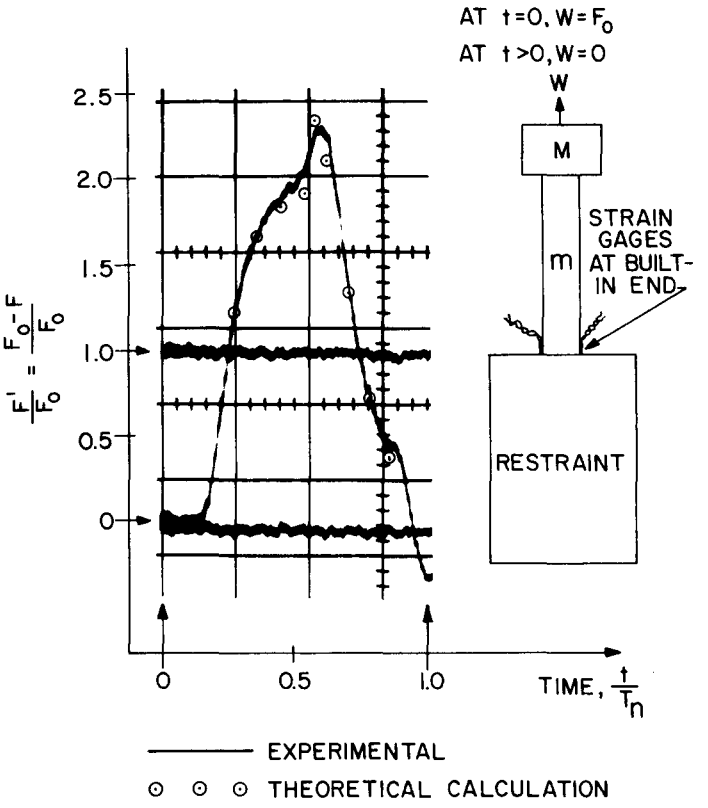

FIG. 14. Comparison of experimental and theoretical results.

behavior of an actual structure become increasingly accurate as the number of spring–masses is increased, for by subdividing the actual structure into more and more spring–masses, the inertia of the structure is more and more accounted for.

REFERENCES

[1] C. H. NORRIS, *et al.*, *Structural Design for Dynamic Loads*. McGraw-Hill (1959).
[2] S. TIMOSHENKO and D. H. YOUNG, *Advanced Dynamics*. McGraw-Hill (1948).
[3] S. TIMOSHENKO, *Vibration Problems in Engineering*, 3rd Edn. Van Nostrand (1955).
[4] J. M. FRANKLAND, Effects of impact on simple-elastic structures, DTMB Report 481 (1942).
[5] A. E. H. LOVE, *A Treatise on the Mathematical Theory of Elasticity*, 4th Edn. Dover (1944).
[6 W. GOLDSMITH, *Impact*. Arnold (1960).
[7] B. D. ST. VENANT and FLAMANT, Resistance vive ou dynamique des solids. Representation graphique des lois du choc longitudinal, *C. r. hebd. Séanc. Acad. Sci., Paris*, 97, 127, 214, 281, and 444 (1883).
[8] R. COURANT and K. O. FRIEDRICHS, *Supersonic Flow and Shock Waves*, Vol. I. Interscience (1948).
[9] G. MOREY, *The Properties of Glass*. Reinhold (1938).

APPENDIX

Rigid mass. A piece of Mallory 1000 Heavymetal (sintered combination of 95 per cent tungsten and 5 per cent Cu–Ni), 0·500 in. in diameter and 0·303 in. thick, weighing 0·0361 lb, $E = 45 \times 10^6$ lb/in.^{2}, $\rho_0 = 1{\cdot}61 \times 10^{-3}$ lb sec^2/in.^{4}

Bar. A glass rod (Corning 7740 Borosilicate), 0·312 in. dia. and 11·98 in. long, weighing 0·0730 lb, $E = 9 \times 10^6$ lb/in.^{2}, $\rho_0 = 2{\cdot}06 \times 10^{-4}$ lb sec^2/in.^{4}
Restraint. A piece of Mallory 1000 Heavymetal, 2·13 in. dia. and 12·62 in. long, weighing 28·0 lb.

The experimental bar–mass system thus had an m/M ratio equal to 2·02. A thin layer of epoxy cement was used to join the components of the system together.

(*Received* 17 *July* 1968; *revised* 20 *January* 1969)

Абстракт—Вместе с экспериментальным подтверждением описывается задача системы стержня и массы. Стерженъ закреплен на одном конце и имеет жесткую массу, связанную с другим концом. Эта масса находится под влиянием прямоугольного ступенчатого импульса силы. Величина этого импульса такова, что вызывает упругую деформацию стержня. Высчитано резулътаты поведения системы стерженъ-масса, предполагая, что напряжения в стержне одномерны. Расчеты указывают на факт, что эта система вызывает усилия значителъно болъшие, чем вызванные эквивалентным приближением пружина-масса, для случая короткого действия импулъса или малой величины массы. Полученные резулътаты подтверждаются экспериментальными полученными на системе стерженъ-масса.